www.editada.org

International Journal of Combinatorial Optimization Problems and Informatics, 18(1), 2027, 60-70. ISSN: 2007-1558.
https://doi.org/10.61467/2007.1558.2027.v18i1.1489

Disturbance Observer-Based Model Predictive Control for a Twin Rotor MIMO System

Nicolas Vite-Vargas[1], Omar Sandre-Hernandez[1,2], Carlos Cuvas-Castillo[3], Jesús-Patricio Ordaz-Oliver[1]

[1] Área Académica de Informática y Electrónica, Universidad Autónoma del Estado de Hidalgo, Hidalgo, México.

[2] Secretaría de Ciencia, Humanidades, Tecnología e Innovación (SECIHTI), Mexico.

[3] Departamento de Ingeniería Mecánica Automotriz, Universidad Politécnica de Pachuca, Hidalgo, México.

Email address(es): vi185412@uaeh.edu.mx, omar_sandre@uaeh.edu.mx, carlos.cuvas@upp.edu.mx, jesus_ordaz@uaeh.edu.mx

✉Corresponding author: Omar Sandre-Hernandez

Abstract. This paper presents a disturbance observer–based model predictive control strategy for the position control of a twin rotor multiple-input multiple-output (MIMO) system (TRMS). The no+nlinear dynamics of the TRMS are first rewritten as an uncertain linear time-invariant (LTI) system with additive disturbances. An extended state observer (ESO) is then designed to estimate both the system states and the lumped disturbance term. Using these estimates, a composite model predictive control law is formulated to achieve robust tracking performance of the desired TRMS positions. Simulation results demonstrate the effectiveness of the proposed control scheme.

Keywords: Disturbance Observer, Model Predictive Control, Twin Rotor.

Article information
Received: Jun 19, 2026
Accepted: Aug 01, 2026

1 Introduction

In recent times, unmanned aerial vehicles (UAV) have attracted significant attention from the control research community. From a control perspective, UAVs present significant challenges. The dynamics of UAVs are nonlinear and exhibit strong coupling between translational and rotational motions. Moreover, UAVs are affected by internal and external disturbances. Among UAVs, the twin rotor MIMO system (TRMS) is a platform that emulates a helicopter and is a classical benchmark for the development of several control schemes.

The TRMS is a two-degree-of-freedom system in which the yaw and pitch movements are driven by two independent rotors. The front (main) rotor generates the pitch motion, while the tail rotor produces the yaw motion, resulting in a nonlinear and strongly coupled MIMO system (Juang et al., 2008). Since the TRMS exhibits aerodynamic nonlinearities, gravitational effects, actuator saturation, and internal coupling between the two axes, it provides a challenging platform for control design.

Several control strategies have been proposed for the TRMS, including PID control (Juang et al., 2008a; Juang et al., 2008b), fuzzy control (Zeghlache et al., 2022), sliding mode control (Palepogu & Mahapatra, 2024; Rashad et al., 2017), backstepping control (Panda et al., 2020), optimal control (Vrazhevsky et al., 2022; Shah et al., 2023), and model predictive control (MPC) (Ebirim et al., 2023; Rahideh & Hasan Shaheed, 2011; Raghavan & Thomas, 2020; Zhao et al., 2026).

Among these control strategies, MPC has become particularly attractive for UAVs. Unlike nonlinear controllers, MPC explicitly handles multivariable systems, actuator constraints, and prediction of future behavior through an optimization-based control approach. For instance, (Ebirim et al., 2023) propose a constrained MPC with integral action. This method guarantees zero steady-state error and accurate reference tracking. In (Rahideh & Hasan Shaheed, 2011), a stable MPC is proposed. In this approach, the MPC solves a quadratic cost function subject to input constraints. In (Raghavan & Thomas, 2020), a Laguerre function-based MPC is introduced to alleviate the computational burden associated with the MPC.

Although these control strategies have demonstrated satisfactory performance, the effectiveness of the MPC strongly depends on the accuracy of the model used for control design. Consequently, its performance may degrade in the presence of external disturbances or parametric uncertainties. An alternative to enhance the robustness of MPC is to use a disturbance observer (DOB), as in (Zhao et al, 2026; Dutta & Das, 2023). These works propose a DOB-based MPC (DOB-MPC), in which the DOB provides an estimate of the disturbance of the system. The resulting DOB-MPC yields a composite control law in which a feedback gain stabilizes the system, while a disturbance compensation term enhances robustness.

This work introduces a DOB-MPC for the position control of a TRMS. First, the nonlinear model of the TRMS is written as an uncertain disturbed system. Then, an extended state observer (ESO) is used to estimate the lumped disturbance of the system, which includes external disturbances, unmodeled dynamics, and parametric uncertainties. By using the estimated disturbance, the MPC problem is formulated as a finite-horizon optimal control problem. A quadratic cost is minimized using dynamic programming, subject to the system dynamics. By incorporating the ESO-estimated disturbance, the MPC provides a robust control design against uncertainties and external disturbances. Simulation results are presented to demonstrate the effectiveness of the proposed control scheme.

2 Theoretical Background

2.1 TRMS dynamics

The free-body diagram of the TRMS is shown in Fig. 1. The system has two degrees of freedom, pitch and yaw, denoted by the generalized coordinates q_1 and q_2, respectively. The main and tail rotors generate the thrust forces $F_1(\omega_1)$ and $F_2(\omega_2)$, which act at the ends of the horizontal beam and generate the torques required to control these angles. Each rotor has an associated mass, denoted m_m for the main rotor and m_T for the tail rotor, and both are affected by gravity g. The beam geometry is characterized by the distances l_m, l_T, and the center-of-mass location l_c, which determine the gravitational torque acting on the pitch axis. Viscous friction at the pitch and yaw joints is modeled by the coefficients b_1 and b_2. This configuration defines the kinematic relationships and external forces used to derive the dynamic model of the TRMS through the Euler-Lagrange formulation.

Using the Euler-Lagrange formulation, the model is expressed in the standard robotic equation:

$$\mathbf{M}(q)\ddot{q} + \mathbf{C}(q,\dot{q})\dot{q} + \mathbf{G}(q) = \mathbf{Q}, \tag{1}$$

where $\mathbf{M}(q)$ is the inertia matrix, $\mathbf{C}(q,\dot{q})$ contains the Coriolis and centrifugal terms, $\mathbf{G}(q)$ is the potential energy force vector, $\mathbf{Q}$ represents the non-potential forces, and $q = [q_1 \quad q_2]^T$. The matrices in (1) are given as follows:

$$\mathbf{M}(q) = \begin{bmatrix} Ml_c^2\cos^2(2q_2) + \mathrm{J} & 0 \\ 0 & Ml_c^2 + \mathrm{J} \end{bmatrix},\ \mathbf{C}(q,\dot{q}) = -Ml_c^2\cos(q_2)\sin(q_2)\begin{bmatrix} \dot{q}_2 & \dot{q}_1 \\ -\dot{q}_1 & 0 \end{bmatrix},$$

$$\mathbf{G}(q) = \begin{bmatrix} Mgl_c\cos(q_1) \\ 0 \end{bmatrix},\ \mathbf{Q} = \begin{bmatrix} (l_c + l_T)F_1(\omega_1) - b_1\dot{q}_1 \\ l_T F_2(\omega_2) - b_2\dot{q}_2 \end{bmatrix},$$

where M is the mass of the TRMS, and J is the moment of inertia. The following state variables are defined: $x_1 = q_1$, $x_2 = q_2$, $x_3 = \dot{q}_1$ and $x_4 = \dot{q}_2$; and the control input is selected as: $u_1 = F_1(\omega_1)$ and $u_2 = F_2(\omega_2)$. Hence, the TRMS dynamics can be written as follows:

$$\dot{x} = f(x) + \mathbf{B}u + \zeta(t), \quad x(0) = x_0, \tag{2}$$

where:

$$f(x) = \begin{bmatrix} x_3 \\ x_4 \\ \dfrac{2Ml_c^2 x_3 x_4\cos(x_2)\sin(x_2) - b_1 x_3}{Ml_c^2\cos(x_2) + \mathrm{J}} \\ \dfrac{-Ml_c^2 x_3^2\cos(x_2)\sin(x_2) - Mgl_c\cos(x_2) - b_2 x_4}{Ml_c^2 + \mathrm{J}} \end{bmatrix},\ \mathbf{B} = \begin{bmatrix} 0 & 0 \\ 0 & 0 \\ \dfrac{l_c + l_T}{Ml_c^2\cos(x_2) + \mathrm{J}} & 0 \\ 0 & \dfrac{l_T}{Ml_c^2 + \mathrm{J}} \end{bmatrix},\ u = \begin{bmatrix} u_1 \\ u_2 \end{bmatrix}.$$

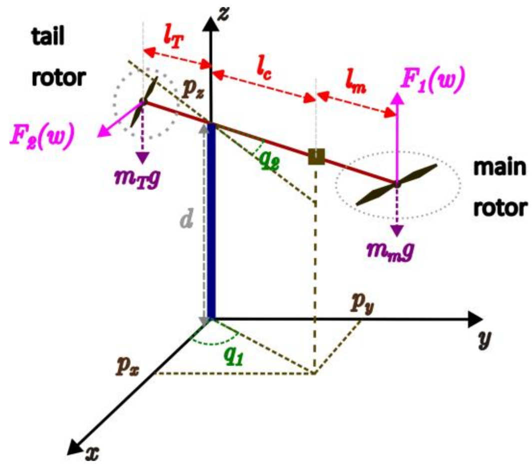

Fig. 1. TRMS free-body diagram.

2.2 Integral MPC (IMPC) of the TRMS

The conventional MPC is introduced in this section and is based on (Ebirim et al., 2023; Rahideh & Hasan Shaheed, 2011; Raghavan & Thomas, 2020). In these works, the MPC is formulated based on an LTI model of the TRMS, and an integral action is embedded to compensate for steady-state errors, leading to the so-called integral model predictive control (IMPC) scheme. Observe that the nonlinear disturbed system given by (2) can be rewritten as (Ordaz et al., 2023):

$$\begin{aligned} \dot{x} &= Ax + Bu + B_d w(t,x,u), \\ w(t,x,u) &= \dot{x} - (Ax + Bu), \\ y &= Cx, \end{aligned} \tag{3}$$

where $w(t,x,u)$ is a lumped disturbance that captures nonlinearities, coupling effects, and unmodeled dynamics. Matrices A and B can be obtained from the linearization around an operating point. In this work, the operating point is selected as $x_d = (\pi/2, \pi/16, 0, 0)$. Then, for system (3), the matrices are given as follows:

$$A = \begin{bmatrix} 0 & 0 & 1 & 0 \\ 0 & 0 & 0 & 1 \\ 0 & 0 & \dfrac{-b_1}{Ml_c^2 + \mathrm{J}} & 0 \\ 0 & \dfrac{Mgl_c}{Ml_c^2 + \mathrm{J}} & 0 & \dfrac{-b_2}{Ml_c^2 + \mathrm{J}} \end{bmatrix}, \; B = \begin{bmatrix} 0 & 0 \\ 0 & 0 \\ \dfrac{l_c + l_T}{Ml_c^2 + \mathrm{J}} & 0 \\ 0 & \dfrac{l_T}{Ml_c^2 + \mathrm{J}} \end{bmatrix}, \; Bd = \begin{bmatrix} 0 & 0 \\ 0 & 0 \\ 1 & 0 \\ 0 & 1 \end{bmatrix},$$

$$w(t,x,u) = \begin{bmatrix} 0 \\ 0 \\ f_3(x) + \mathbf{B}_{31}(x_2)u_1 + \dfrac{b_1}{Mlc^2 + \mathrm{J}}x_3 - \dfrac{l_c + l_T}{Ml_c^2 + \mathrm{J}}u_1 \\ \dfrac{-Ml_c^2 x_3^2 \cos(x_2)\sin(x_2)}{Ml_c^2 + \mathrm{J}} - \dfrac{Mgl_c}{Ml_c^2 + \mathrm{J}}\left(\cos(x_2) + x_2\right) \end{bmatrix}, \; f_3(x) = \frac{2Ml_c^2 x_3 x_4 \cos(x_2)\sin(x_2) - b_1 x_3}{Ml_c^2 \cos(x_2) + \mathrm{J}},$$

$$\mathbf{B}_{31}(x_2) = \frac{l_c + l_T}{Ml_c^2 \cos(x_2) + \mathrm{J}}, \; C = \begin{bmatrix} 1 & 0 & 0 & 0 \\ 0 & 1 & 0 & 0 \end{bmatrix}.$$

For the MPC design, the system in (3) is discretized using the Euler method. Since the lumped disturbance is unknown, it is not included in the MPC prediction model. Instead, an integrator is embedded in the discrete-time formulation to mitigate its effect on the system response. The resulting augmented discrete-time model is given by (Wang, 2009):

$$\underbrace{\begin{bmatrix} \Delta x_{k+1} \\ y_{k+1} \end{bmatrix}}_{x_{m_{k+1}}} = \underbrace{\begin{bmatrix} G & 0^T \\ CG & I_{p\times p} \end{bmatrix}}_{A_m} \underbrace{\begin{bmatrix} \Delta x_k \\ y_k \end{bmatrix}}_{x_{m_k}} + \underbrace{\begin{bmatrix} H \\ CH \end{bmatrix}}_{B_m} \Delta u_k, \tag{4}$$

$$y_k = \underbrace{\begin{bmatrix} 0 & I_{p\times p} \end{bmatrix}}_{C_m} \begin{bmatrix} \Delta x_k \\ y_k \end{bmatrix},$$

where $\Delta x_k = x_k - x_{k-1}$, $\Delta u_k = u_k - u_{k-1}$, $G = I + AT_s$, $H = BT_s$, T_s is the sampling time, p is the number of outputs, and 0_m denotes a zero matrix of appropriate dimensions. For the augmented system given by (4), the objective of the MPC is to design the optimal control sequence over a prediction horizon N, given by:

$$\Delta U = \left[\Delta u_k, \Delta u_{k+1}, ..., \Delta u_{k+N-1}\right]^T.$$

Then, the MPC is designed as:

$$\begin{aligned} &\min_{\Delta U} \sum_{k=0}^{N-1} \|r - y_k\|_Q^2 + \|\Delta u_k\|_R^2 \\ &\text{s.t.} \\ &u_{\min} \le u_{k-1} + \Delta u_k \le u_{\max}, \quad k = 0,\dots,N-1 \\ &x_{m_{k+1}} = A_m x_{m_k} + B_m \Delta u_k, \quad k = 0,\dots,N-1 \\ &y_k = C_m x_{m_k} \\ &x_{m_0} = x_0. \end{aligned} \tag{5}$$

In (5), $\|x\|_M^2 \triangleq x^T M x$, $Q \geq 0$ and $R > 0$. The matrix Q regulates the deviation from the reference, while R penalizes the applied control effort. $u_{\min}$ and $u_{\max}$ define the minimum and maximum admissible values of the control input. To solve (5), a quadratic programming method is used, and the final control action is obtained based on the principle of receding-horizon control as:

$$u_k = u_{k-1} + \overbrace{\left[I\, 0 \dots 0\right]}^{N_p} \Delta U^*,$$

where the notation * denotes the optimal solution of (5).

3 Disturbance Observer-based Model Predictive Control

The integral action of the conventional IMPC provides a degree of robustness against disturbances in the TRMS. In particular, constant disturbances are rejected from the TRMS response using this approach; however, for time-varying disturbances, the integral action only mitigates their effect on the system response. This limitation motivates the use of a DOB-MPC. In the proposed approach, the lumped disturbance of the TRMS is estimated and actively compensated through a composite control law that combines the disturbance estimate with the predictive capabilities of MPC.

3.1 Disturbance Observer

Consider the following discrete-time model of the TRMS:

$$\begin{aligned} x_{k+1} &= Gx_k + Hu_k + B_{dd} d_k, \\ y_k &= Cx_k, \end{aligned} \tag{6}$$

where $B_{dd} = B_d T_s$ and d_k is the lumped disturbance of the TRMS. The state and disturbance in the TRMS are estimated using an ESO. These estimates are used to initialize the MPC problem. It is assumed that the lumped disturbance is bounded and slowly time-varying, which is represented in discrete-time by the model $d_{k+1} = d_k$. This ensures that the disturbance does not change abruptly between sampling instants. The following DOB is considered (Maeder et al., 2009):

$$\hat{x}_{k+1} = G\hat{x}_k + Hu_k + B_{dd}\hat{d}_k + L_x(y_k - \hat{y}_k),$$
$$\hat{d}_{k+1} = \hat{d}_k + L_d(y_k - \hat{y}_k),$$
$$\hat{y}_k = C\hat{x}_k.$$

Where $\hat{x}$ and $\hat{d}$ are the state and disturbance estimates, respectively, and L_x and L_d are the observer gains. By defining the state estimation error as $e_{x_k} = x_k - \hat{x}_k$, the disturbance estimation error as $e_{d_k} = d_k - \hat{d}_k$, and the extended observation error as $e_k = [e_{x_k} \quad e_{d_k}]^T$, the DOB error dynamics are given by:

$$e_{k+1} = \left(\begin{bmatrix} G & Bdd \\ 0 & I \end{bmatrix} - \begin{bmatrix} L_x \\ L_d \end{bmatrix} \begin{bmatrix} C & 0 \end{bmatrix} \right) e_k.$$

And the stability of the estimation error depends on the appropriate selection of the observer gains L_x and L_d.

3.2 DOB-MPC

An MPC in which disturbance estimation is incorporated into the optimization problem is proposed. Based on (6), the current state x_k, and the current disturbance estimate $\hat{d}_k$, the objective of the DOB-MPC is to design the optimal control sequence over a prediction horizon N, given by:

$$U = \left[u_k, u_{k+1}, \ldots, u_{k+N-1}\right]^T.$$

Then, the following optimization problem for the position control of the TRMS is formulated:

$$\begin{aligned} &\min_U \|r - y_N\|_P^2 + \sum_{k=0}^{N-1} \|r - y_k\|_Q^2 + \|u_k\|_R^2 \\ &\text{s.t.} \\ &x_{k+1} = Gx_k + Hu_k + B_{dd}d_k \quad k = 0, \ldots, N-1 \\ &d_{k+1} = d_k \\ &y_k = Cx_k \\ &x_0 = x_k \\ &d_0 = \hat{d}_k. \end{aligned} \tag{7}$$

Where $Q \geq 0$, $R > 0$, and P satisfy the discrete-time Riccati equation. Although the optimization is initialized with x_k and $\hat{d}_k$, this does not correspond to solving a fixed-window problem. The controller still follows the receding-horizon principle: at each sampling instant, the optimization is solved using the updated measurements, and only the first input of the optimal sequence is applied.

The optimization problem introduced in (7) is solved using dynamic programming. Based on the cost function, the terminal cost $J_N(x_N)$ and stage cost $L_k(x_k, u_k)$ are defined as follows:

$$J_N(x_N) = (r - y_N)^T P(r - y_N),$$
$$L_k(x_k, u_k) = (r - y_k)^T Q(r - y_k) + u_k^T R u_k.$$

The optimal cost-to-go $J_k(x_k)$ is defined as the minimum cost from stage k to the terminal stage N, starting from the state x_k, and is given by:

$$J_k(x_k) = \min_{u_k}\left(L_k(x_k, u_k) + J_{k+1}(x_{k+1})\right).$$

According to the principle of optimality, the cost-to-go at stage $N-1$ is:

$$
\begin{aligned}
&J_{N-1}^{*}(x_{N-1}) = \min_{u_{N-1}} \left(L_{N-1}(x_{N-1}, u_{N-1}) + J_{N}(x_{N}) \right) \\
&\text{s.t.} \\
&x_{N} = Gx_{N-1} + Hu_{N-1} + B_{dd}\hat{d}_{N-1} \\
&y_{N-1} = Cx_{N-1} \\
&P_{N} = P.
\end{aligned}
$$

It is noted that the cost-to-go $J_{N-1}(x_{N-1})$ is a positive definite quadratic function; hence, the optimal control u_{N-1}^{*} is obtained when $\partial J_{N-1}(x_{N-1}) / \partial u_{N-1} = 0$ as:

$$
u_{N-1}^{*} = \left(R + H^{\bullet} C^{\bullet} P_{N} CH \right)^{-1} \left[H^{\bullet} C^{\bullet} P_{N} r - H^{\bullet} C^{\bullet} \left(P_{N} CGx_{N-1} + P_{N} CB_{dd} \hat{d}_{N-1} \right) \right].
$$

By substituting the optimal control law u_{N-1}^{*} back into the cost-to-go function, the minimum cost at stage $N-1$ can be expressed in the standard quadratic form as:

$$
J_{N-1}^{*}(x_{N-1}) = x_{N-1}^{\bullet} S_{N-1} x_{N-1} + 2 s_{N-1}^{\bullet} x_{N-1} + c_{N-1},
$$

where

$$
\begin{aligned}
S_{N-1} &= G^{\bullet} C^{\bullet} P_{N} CG + C^{\bullet} QC - G^{\bullet} C^{\bullet} P_{N} CH \left(R + H^{\bullet} C^{\bullet} P_{N} CH \right)^{-1} H^{\bullet} C^{\bullet} P_{N} CG, \\
s_{N-1}^{\bullet} &= -r^{\bullet} P_{N} CG - r^{\bullet} QC + \hat{d}_{N-1}^{\bullet} B_{dd}^{\bullet} C^{\bullet} P_{N} CG - \hat{d}_{N-1}^{\bullet} B_{dd}^{\bullet} C^{\bullet} P_{N} CH \left(R + H^{\bullet} C^{\bullet} P_{N} CH \right)^{-1} H^{\bullet} C^{\bullet} P_{N} CG \\
&\quad + r^{\bullet} P_{N} CH \left(R + H^{\bullet} C^{\bullet} P_{N} CH \right)^{-1} H^{\bullet} C^{\bullet} P_{N} CG, \\
c_{N-1} &= r^{\bullet} P_{N} r + r^{\bullet} Qr - 2r^{\bullet} P_{N} CB_{dd} \hat{d}_{N-1} \\
&\quad - \left(C^{\bullet} P_{N} CB_{dd} \hat{d}_{N-1} - C^{\bullet} P_{N} r \right)^{\bullet} H \left(R + H^{\bullet} C^{\bullet} P_{N} CH \right)^{-1} H^{\bullet} \left(C^{\bullet} P_{N} CB_{dd} \hat{d}_{N-1} - C^{\bullet} P_{N} r \right).
\end{aligned}
$$

The derivation presented for stage $N-1$ can be generalized to any stage k of the prediction horizon. To this end, the optimal cost-to-go at stage $k+1$ is written as:

$$
J_{k+1}^{*}(x_{k+1}) = x_{k+1}^{\bullet} S_{k+1} x_{k+1} + 2 s_{k+1}^{\bullet} x_{k+1} + c_{k+1}.
$$

Using Bellman's principle of optimality:

$$
J_{k}^{*}(x_{k}) = \min_{u_{k}} \left(L_{k}(x_{k}, u_{k}) + J_{k+1}^{*}(x_{k+1}) \right), \tag{8}
$$

with $x_{k+1} = Gx_{k} + Hu_{k} + B_{dd}\hat{d}_{k}$ and $y_{k} = Cx_{k}$, the optimal control input at stage k is obtained as:

$$
u_{k}^{*} = K_{r_{k}} r - K_{x_{k}} x_{k} - K_{d_{k}} \hat{d}_{k}, \tag{9}
$$

with

$$
\begin{aligned}
K_{x_{k}} &= \left(R + H^{\bullet} C^{\bullet} S_{k+1} CH \right)^{-1} H^{\bullet} C^{\bullet} S_{k+1} CG, \\
K_{r_{k}} &= \left(R + H^{\bullet} C^{\bullet} S_{k+1} CH \right)^{-1} H^{\bullet} C^{\bullet} S_{k+1}, \\
K_{d_{k}} &= \left(R + H^{\bullet} C^{\bullet} S_{k+1} CH \right)^{-1} H^{\bullet} C^{\bullet} S_{k+1} CB_{dd}.
\end{aligned}
$$

By substituting u_{k}^{*} back into (8), the optimal cost-to-go at stage k is:

$$
J_{k}^{*}(x_{k}) = x_{k}^{\bullet} S_{k} x_{k} + 2 s_{k}^{\bullet} x_{k} + c_{k},
$$

where the matrices S_{k}, s_{k}, and c_{k} satisfy the backward recursions

Algorithm 1. Offline computation of the backward recursions for DOB-MPC

Input: Prediction horizon N, matrices G, H, C, B_{dd}, weights Q,

R, P

Output: Gains K_{x_k}, K_{r_k}, K_{d_k} for $k = 0, \ldots, N-1$

Initialization:

$S_N \leftarrow C^T PC$

$s_N \leftarrow -C^T \Pr$

$c_N \leftarrow r^T \Pr$

for $k = N-1$ **to** 0 **do**

Compute the control gains from (9):

$K_{x_k} \leftarrow \left(R + H^{\bullet} C^{\bullet} S_{k+1} CH\right)^{-1} H^{\bullet} C^{\bullet} S_{k+1} CG$

$K_{r_k} \leftarrow \left(R + H^{\bullet} C^{\bullet} S_{k+1} CH\right)^{-1} H^{\bullet} C^{\bullet} S_{k+1}$

$K_{d_k} \leftarrow \left(R + H^{\bullet} C^{\bullet} S_{k+1} CH\right)^{-1} H^{\bullet} C^{\bullet} S_{k+1} CB_{dd}$

$S_k \leftarrow$ expression in (10)

$s_k \leftarrow$ expression in (11)

$c_k \leftarrow$ expression in (12)

Return: K_{x_0}, K_{r_0}, K_{d_0} for online implementation.

$$S_k = G^{\bullet} C^{\bullet} S_{k+1} CG + C^{\bullet} QC - G^{\bullet} C^{\bullet} S_{k+1} CH\left(R + H^{\bullet} C^{\bullet} S_{k+1} CH\right)^{-1} H^{\bullet} C^{\bullet} S_{k+1} CG, \tag{10}$$

$$\begin{aligned} s_k^{\bullet} &= -r^{\bullet} S_{k+1} CG - r^{\bullet} QC + \hat{d}_k^{\bullet} B_{dd}^{\bullet} C^{\bullet} S_{k+1} CG - \hat{d}_k^{\bullet} B_{dd}^{\bullet} C^{\bullet} S_{k+1} CH\left(R + H^{\bullet} C^{\bullet} S_{k+1} CH\right)^{-1} \\ &\times H^{\bullet} C^{\bullet} S_{k+1} CG + r^{\bullet} S_{k+1} CH\left(R + H^{\bullet} C^{\bullet} S_{k+1} CH\right)^{-1} \times H^{\bullet} C^{\bullet} S_{k+1} CG, \end{aligned} \tag{11}$$

$$\begin{aligned} c_k &= r^{\bullet} S_{k+1} r + r^{\bullet} Qr - 2r^{\bullet} S_{k+1} CB_{dd} \hat{d}_k - \left(C^{\bullet} S_{k+1} CB_{dd} \hat{d}_k - C^{\bullet} S_{k+1} r\right)^{\bullet} \\ &\times H\left(R + H^{\bullet} C^{\bullet} S_{k+1} CH\right)^{-1} H^{\bullet} \left(C^{\bullet} S_{k+1} CB_{dd} \hat{d}_k - C^{\bullet} S_{k+1} r\right). \end{aligned} \tag{12}$$

For any stage k, the set of backward recursions is similar to the discrete-time Riccati equation. Moreover, since the matrices (G, H, C, B_{dd}) and the weighting matrices (Q, P, R) are time-invariant, the solution of the backward recursions given by (10)-(12), can be solved offline. This procedure is detailed in Algorithm 1.

4 Simulation Results

The performance of the proposed DOB-MPC is evaluated through numerical simulations in MATLAB. The control objective is to track the desired pitch and yaw angles of the TRMS. The parameters of the TRMS are listed in Table 1. To evaluate the advantages of the proposed approach, a comparative study is conducted between the conventional IMPC described in Section 2.2 and the proposed DOB-MPC. Both controllers are implemented under identical conditions, including actuator constraints (DOB-MPC includes actuator saturation in the control action), sampling time, prediction horizon, penalty matrices, and reference trajectories. These parameters are also listed in Table 1.

Table 1. Parameters of the TRMS used in simulation.

Parameter	Symbol	Value
Mass	M	0.3 kg
Center-of-mass distance	l_c	0.25 m
Tail rotor distance	l_T	−0.29 m
Moment of inertia	J	0.0072 kg・m^2
Gravity	g	9.81 m/s^2
Pitch viscous friction	b_1	0.0984
Yaw viscous friction	b_2	0.0983
Sampling time	T_s	0.001 s
Prediction horizon	N	100
Output weighting	Q	diag(10^4, 10^6)
Terminal weighting	P	diag(10^7, 10^7)
Input weighting	R	diag(50, 10)
Input constraints	$u_{\min}, u_{\max}$	[−15, 15]

The performance of the controllers is evaluated under two reference-tracking scenarios. For the first test, the pitch angle reference is set to 0 rad at 0s, then at 2s it is changed to $\pi/6$, and at 6s it is changed to $-\pi/6$. The setpoint for the yaw angle is 0 rad at 0s, then at 3s it is changed to $\pi/6$, and at 7s it is changed to $-\pi/6$. In the second scenario, a time-varying circular reference is used to simultaneously excite both axes. The pitch reference is defined as $0.3\,cos(0.4t)$, and the yaw reference as $0.3\,sin(0.4t)$.

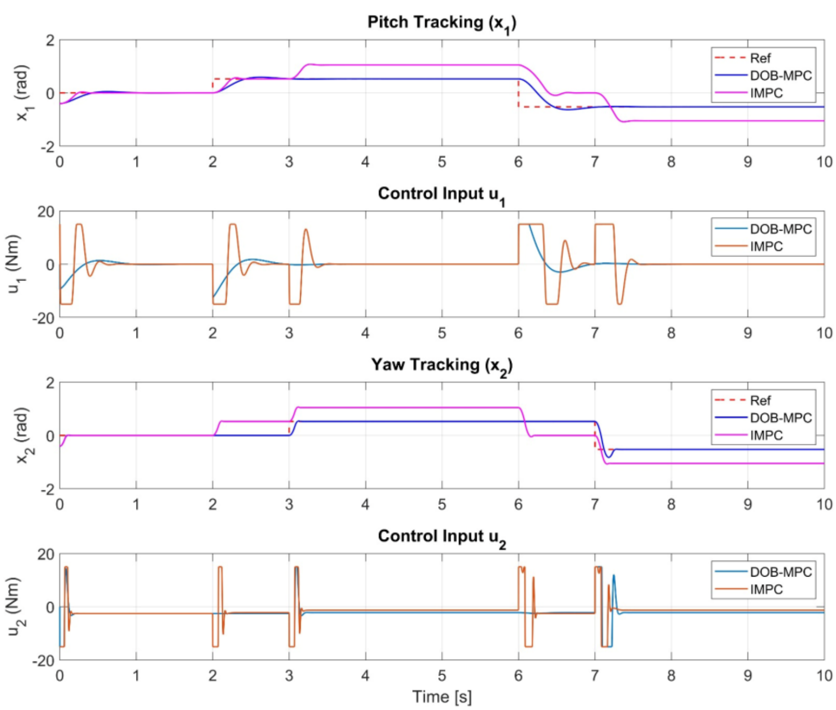

Fig. 2. Tracking performance of IMPC and DOB-MPC under constant reference signals. From top to bottom: Pitch angle tracking (x_1), Pitch control input (u_1), Yaw angle tracking (x_2), Yaw control input (u_2).

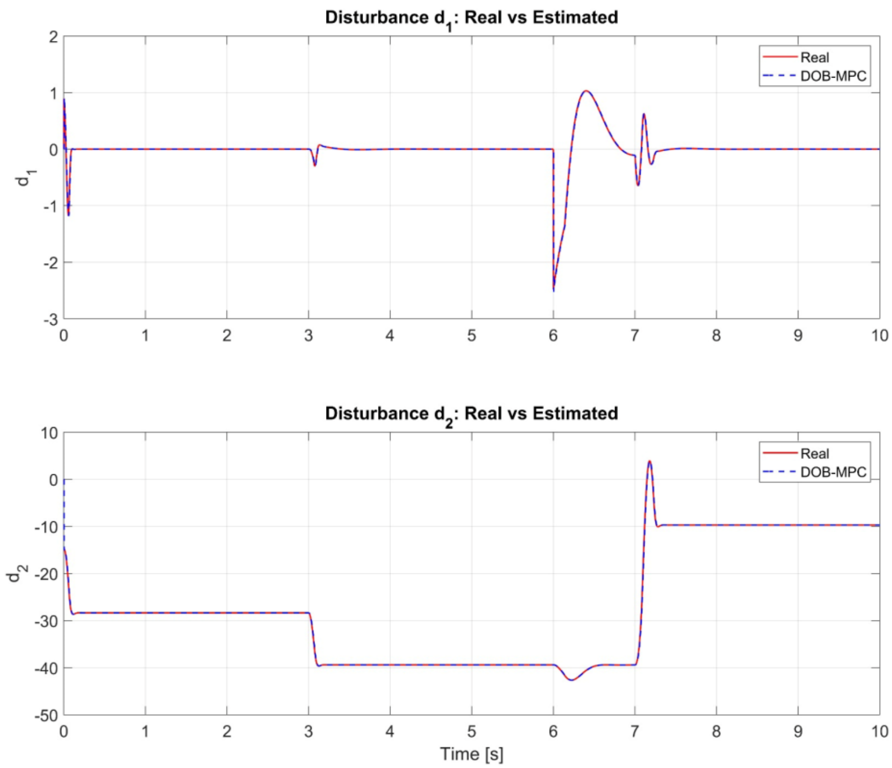

Fig. 3. Real and estimated lumped disturbances under constant reference tracking. From top to bottom: Pitch disturbance (d_1), Yaw disturbance (d_2).

The simulation results of the first scenario are shown in Fig. 2 and Fig. 3. Fig. 2 shows the reference tracking of the desired pitch and yaw angles. The proposed DOB-MPC achieves improved tracking performance, whereas the conventional IMPC struggles to follow the reference when the operating point deviates significantly from the linearization point of the system. The estimated disturbances are shown in Fig. 3, where the ESO successfully reconstructs the lumped disturbance.

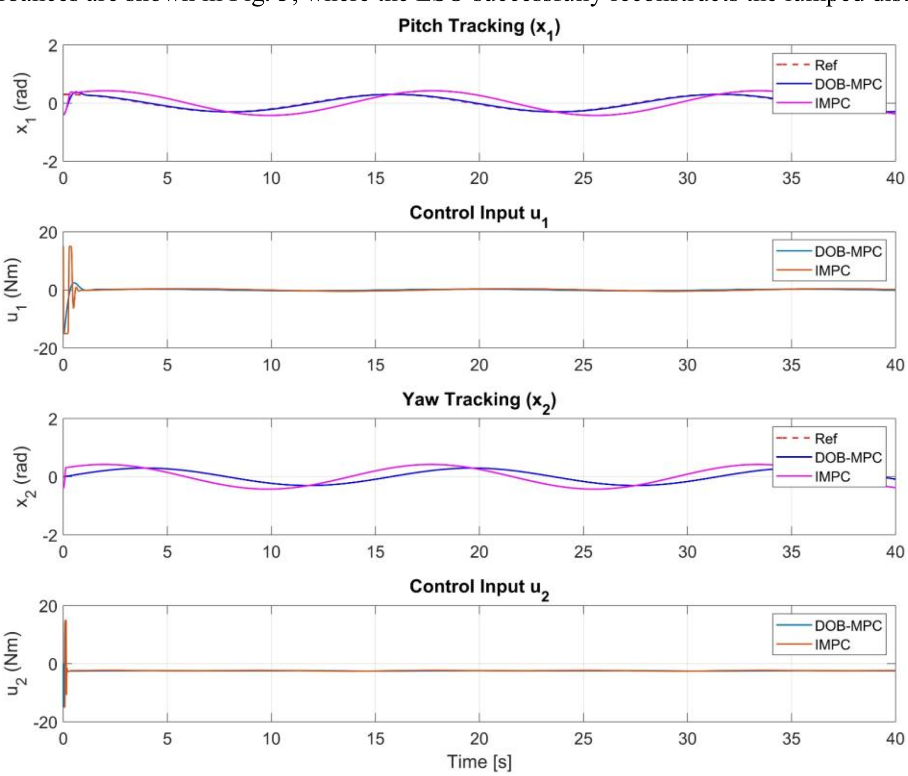

Fig. 4. Tracking performance of IMPC and DOB-MPC under a time-varying circular reference trajectory. From top to bottom: Pitch angle tracking (x_1), Pitch control input (u_1), Yaw angle tracking (x_2), Yaw control input (u_2).

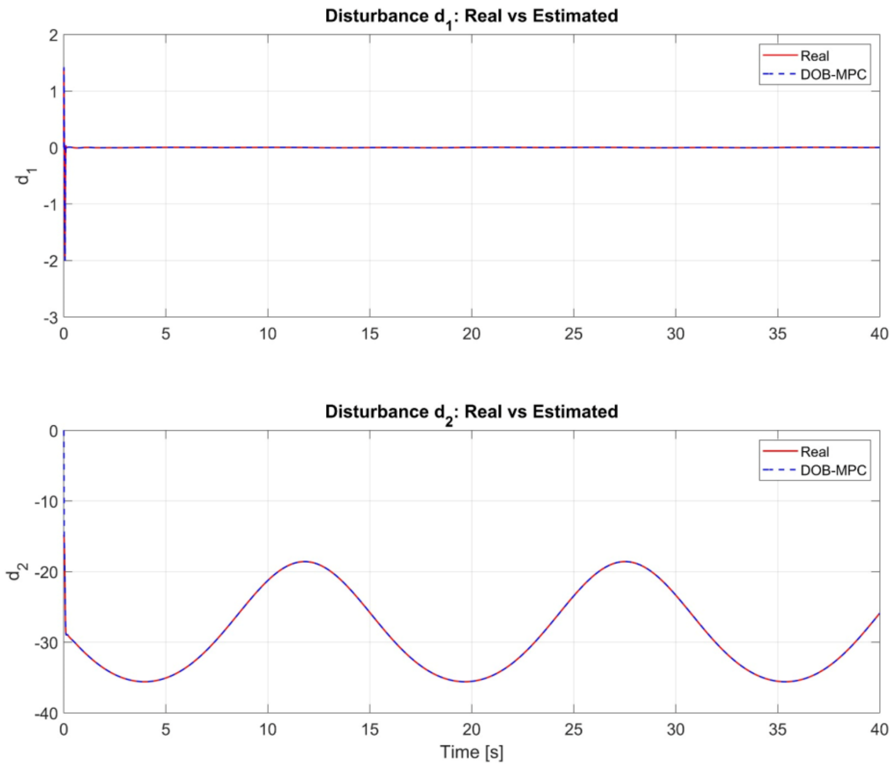

Fig. 5. Real versus estimated lumped disturbances under time-varying circular reference tracking. From top to bottom: Pitch disturbance (d_1), Yaw disturbance (d_2).

The results of the second scenario are shown in Fig. 4 and Fig. 5. Fig. 4 shows the reference tracking of the desired pitch and yaw angles. The proposed DOB-MPC successfully follows the time-varying circular reference. On the other hand, the conventional IMPC struggles to follow the reference, resulting in a significant tracking error. The estimated disturbances are shown in Fig. 5, where the DOB accurately reconstructs the lumped disturbances.

The simulation results, shown in Fig. 2 and Fig. 4, demonstrate that the performance of the conventional IMPC exhibits a noticeable degradation when the TRMS operates far from the linearization point. In contrast, incorporating the disturbance estimate into the control problem enhances robustness and improves the tracking performance of the proposed DOB-MPC.

5 Conclusions

This article presents the integration of a DOB-MPC scheme for the TRMS. The proposed control scheme improves the tracking performance and robustness of the TRMS compared to a conventional IMPC. The model used in MPC incorporates the disturbances estimates, data obtained successfully through the ESO, leading to improved control. The simulation results demonstrate that the proposed approach is effective for nonlinear systems subject to uncertainties, unmodeled dynamics and external disturbances.

Acknowledgements

The authors thank the Ministry of Science, Humanities, Technology and Innovation (SECIHTI), Mexico, for the doctoral scholarship awarded to the first author of this paper, No. 4052738. Part of this work was carried out using AI. Microsoft Copilot was used to assist with preliminary drafting, text consistency checks, and automatic LaTeX code generation for some equations.

References

Dutta, L., & Das, D. K. (2023). Nonlinear disturbance observer based adaptive explicit nonlinear model predictive control design for a class of nonlinear MIMO system. *IEEE Transactions on Aerospace and Electronic Systems, 59*(2), 1965–1979. https://doi.org/10.1109/TAES.2022.3211252

Ebirim, K. U., Lecchini-Visintini, A., Rubagotti, M., & Prempain, E. (2023). Constrained model predictive control with integral action for twin rotor MIMO systems. *Journal of Dynamic Systems, Measurement, and Control, 145*(8), 081006. https://doi.org/10.1115/1.4062735

Juang, J.-G., Huang, M.-T., & Liu, W.-K. (2008). PID control using presearched genetic algorithms for a MIMO system. *IEEE Transactions on Systems, Man, and Cybernetics, Part C (Applications and Reviews), 38*(5), 716–727. https://doi.org/10.1109/TSMCC.2008.923890

Juang, J.-G., Lin, R.-W., & Liu, W.-K. (2008). Comparison of classical control and intelligent control for a MIMO system. *Applied Mathematics and Computation, 205*(2), 778–791. https://doi.org/10.1016/j.amc.2008.05.061

Maeder, U., Borrelli, F., & Morari, M. (2009). Linear offset-free model predictive control. *Automatica, 45*(10), 2214–2222. https://doi.org/10.1016/j.automatica.2009.06.005

Ordaz, P., Alazki, H., Sánchez, B., & Ordaz-Oliver, M. (2023). On the finite time stabilization via robust control for uncertain disturbed systems. *International Journal of Applied Mathematics and Computer Science, 33*(1), 71–82. https://doi.org/10.34768/amcs-2023-0006

Palepogu, K. R., & Mahapatra, S. (2024). Design of sliding mode control with state varying gains for a benchmark twin rotor MIMO system in horizontal motion. *European Journal of Control, 75*, 100909. https://doi.org/10.1016/j.ejcon.2023.100909

Panda, M., Peyada, N. K., & Ghosh, A. (2020). Saturated adaptive backstepping control of uncertain nonlinear systems with validation using twin rotor system. *Journal of the Franklin Institute, 357*(18), 13477–13510. https://doi.org/10.1016/j.jfranklin.2020.10.003

Raghavan, R., & Thomas, S. (2020). Exponentially weighted Laguerre function based model predictive controller for a twin rotor MIMO system. In *2020 International Conference on Power, Instrumentation, Control and Computing (PICC)* (pp. 1–6). IEEE. https://doi.org/10.1109/PICC51425.2020.9362349

Rahideh, A., & Shaheed, M. H. (2011). Stable model predictive control for a nonlinear system. *Journal of the Franklin Institute, 348*(8), 1983–2004. https://doi.org/10.1016/j.jfranklin.2011.05.015

Rashad, R., El-Badawy, A., & Aboudonia, A. (2017). Sliding mode disturbance observer-based control of a twin rotor MIMO system. *ISA Transactions, 69*, 166–174. https://doi.org/10.1016/j.isatra.2017.04.013

Shah, A. Q., Awais, M., Zafar, M., Ahmed, A., Mudassar, M., Muneer, M., Saif, M., Razzaq, A., Jang, S.-H., Kim, S., & Park, Y. (2023). A comparative study of linear control strategies on the aerodynamics twin rotor system. *Journal of Mechanical Science and Technology, 37*(8), 4301–4310. https://doi.org/10.1007/s12206-023-0746-5

Vrazhevsky, S., Kopysova, E., & Kuznetsov, M. (2022). Nonlinear suboptimal robust control for twin rotor MIMO system. In *2022 6th Scientific School Dynamics of Complex Networks and Their Applications (DCNA)* (pp. 303–306). IEEE. https://doi.org/10.1109/DCNA56428.2022.9923275

Wang, L. (2009). *Model predictive control system design and implementation using MATLAB®*. Springer. https://doi.org/10.1007/978-1-84882-331-0

Zeghlache, S., Benyettou, L., Djerioui, A., & Ghellab, M. Z. (2022). Twin rotor MIMO system experimental validation of robust adaptive fuzzy control against wind effects. *IEEE Systems Journal, 16*(1), 409–419. https://doi.org/10.1109/JSYST.2020.3034993

Zhao, J., Liu, S., Xue, W., Ding, Y., & Li, D. (2026). Disturbance-rejection guaranteed MPC design for MIMO systems with application to a 2-DOF helicopter. *Aerospace Science and Technology, 168*, 110757. https://doi.org/10.1016/j.ast.2025.110757